Journal of Materials Chemistry C

Accepted Manuscript

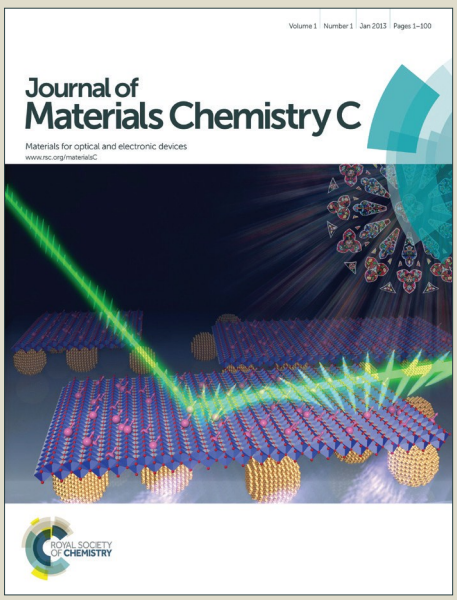

ROYAL SOCIETY OF CHEMISTRY

www.rsc.org/materialsC

Journal of Materials Chemistry C

Journal of Materials Chemistry C

Dynamic Article Links ►

Cite this: DOI: 10.1039/c0xx00000x

www.rsc.org/xxxxxx

Communication

Colored, see-through perovskite solar cells employing an optical cavity

Kyu-Tae Lee,[a,‡] Masanori Fukuda,[a,‡] Suneel Joglekar,[a] and L. Jay Guo[a,*]

Received (in XXX, XXX) Xth XXXXXXXXX 20XX, Accepted Xth XXXXXXXXX 20XX
DOI: 10.1039/b000000x

Multi-functional solar cells that can create semitransparency or desired colors have recently garnered much attention due to their potential in incorporating aesthetic functionalities into building envelopes, such as windows, facades, and walls, allowing large surfaces of the buildings to be utilized for light-harvesting. Here, we present optical microcavity-embedded decorative perovskite solar cells producing distinctive transmissive colors. Any individual semitransparent colors can be created by strong interference effects in the microcavity system, which are easily tuned by changing the thickness of the optical spacer layer of the microcavity. Our colored cell devices show the power conversion efficiency of up to ~4% with high internal quantum efficiency that is attributed to a greatly minimized charge carrier recombination. The approach could bring us one step closer towards energy-saving ultra-thin color display devices and power generating panels for building decoration.

Introduction

Recently, perovskite semiconductors have emerged as a highly attractive photovoltaic (PV) material due to their ability to be fabricated via solution process at low temperatures and with low cost, offering clear advantages over the conventional inorganic PV platforms. In addition, their properties are similar to the inorganic materials, thus being able to achieve high performances. Particularly, considerable attention has been given to the organolead halide perovskite material $CH_3NH_3PbI_{3-x}Cl_x$ that shows strong optical absorption characteristics over a wide range of visible spectrum, and high power conversion efficiency has been achieved even in a simple planar device structure. The thickness of the semiconducting perovskite films used in previous reports is typically a few hundred nanometers so that the majority of the visible lights can be fully absorbed by the photoactive layer for generating large amounts of electricity.[1-11] However such a thick photoactive layer always leads to a black appearance that is not visually attractive, and only suitable for a rooftop installation with limited area, especially for modern high-rise building, while a large number of building envelopes, such as facades, skylights, walls, and windows, cannot be efficiently used for light-harvesting. In order to achieve a semitransparent characteristic, the semiconductor layer thickness has to be greatly reduced. However, the resulting color of a thinner perovskite film has a dark brown color with a reddish tint, very limited in terms of producing visually appealing PV panels.[12]

In PV applications, aesthetic features of PV cells have attracted significant interest due to increasing needs for building-integrated PV (BIPV) that can be harmoniously integrated with the building envelopes. Driven by these strong demands, an organic PV device structure integrated with plasmonic color filters was developed to create desired reflective colors and simultaneously generate the electric power.[13] However the resulting PV cells can produce the colors only at a certain angle and also work for a specific polarization, both of which are attributed to the inherent property of the surface plasmon resonance. To address these challenges, amorphous silicon (a-Si) based hybrid PV cells exploiting strong interference effects in an ultra-thin a-Si active layer and able to create a wide range of transmission and reflection colors have recently been demonstrated.[14-16] In particular, the incident angle and polarization insensitive performances have been achieved by zeroing the optical phases of propagation and reflections.[17-20] In this configuration, the a-Si layer functions as an optical cavity medium as well as photoactive layer, and therefore, the thickness of the a-Si film was limited up to 31 nm so as to make an optical resonance at visible frequency. However, the power conversion efficiency is limited by the ultra-thin thickness of the photoactive layer and achieving a very thin and smooth a-Si layer could be challenging. In fabrication, plasma-enhanced chemical vapor deposition (PECVD) process needs to be used to deposit a-Si. Therefore, a new scheme that can create aesthetic functionalities and PV performance enhancements with solution processability is strongly desirable for large area decorated PV application.

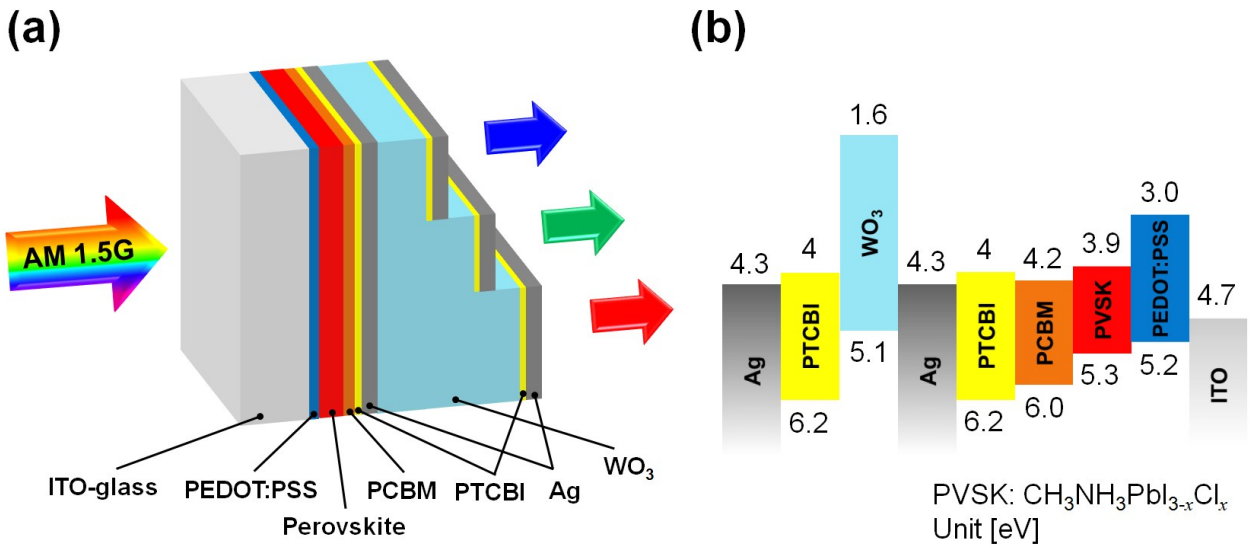

Fig. 1 (a) A schematic view of the proposed colored, semitransparent perovskite PV device employing a microcavity consisting of a dielectric medium sandwiched by optically thin metallic layers in the cathode side. The desired transmission RGB colors can be tuned by simply altering the thickness of the dielectric layer in the microcavity. Each layer's thickness is as follows: PEDOT:PSS=50 nm, Perovskite=80 nm, PCBM=60 nm, Ag=20 nm, PTCBI=8 nm, WO_3=65 (Blue), 85 (Green), 115 nm (Red). (b) Energy level diagram of each layer in the proposed device structure. The energy level is relative to the vacuum level. PVSK represents $CH_3NH_3PbI_{3-x}Cl_x$ and the unit is electron volt (eV).

In this work, we demonstrate colored and semitransparent perovskite PV cells by adopting an optical microcavity configuration where two optically thin metallic layers separated by a dielectric film are employed as a cathode. Simply altering the thickness of the dielectric layer inside such a composite cathode structure enables the resonance transmission of certain wavelength of visible lights (e.g., transmitting red, green, and blue (RGB) colors), without impacting the charge collections by the electrode. In this proposed device structures the non-transmitted portion of the incident light is reflected back to the perovskite material and leads to a strong optical field in the photoactive layer at these complementary spectral regions that improve the photocurrent generation. We also show that the majority of the incident photons absorbed by the perovskite photoactive layer are effectively collected by the electrode due to the thin perovskite film thickness (~80 nm) that is much shorter than a charge diffusion length in the perovskite material, thus leading to highly suppressed charge carrier recombination. The presented scheme offers an appealing path towards decorative BIPV and energy-efficient e-media.

Results and discussion

Fig. 1 (a) presents a schematic diagram of the proposed colored perovskite PV device structure: glass/ITO/poly(3,4-ethylenedioxythiophene):poly(styrenesulfonate) (PEDOT:PSS)/$CH_3NH_3PbI_{3-x}Cl_x$/phenyl-C_{61}-butyric acid methyl ester (PCBM)/perylenetetracarboxylic bis-benzimidazole (PTCBI)/Ag/ tungsten trioxide (WO_3)/PTCBI/Ag. The details of a device fabrication are given in the Experimental Section. Here, PEDOT:PSS, $CH_3NH_3PbI_{3-x}Cl_x$ and PCBM correspond to p-, i- and n- layers, respectively, and a planar p-i-n structure is constructed by layer-by-layer deposition. The thickness of the perovskite layer is 80 nm, allowing some portions of incident light to pass through to reach the microcavity cathode, which will be utilized for creating transmitted R, G, B colors. Ag/WO_3/Ag, a metal-dielectric-metal (MDM) multilayer structure, is utilized not only as a semitransparent electrode[21-26] but also functions as a Fabry-Perot optical cavity to transmit a certain portion of the incident solar spectrum tuned easily by the thickness of the WO_3 layer. We note that the expected power conversion efficiency would be lower than what has been reported as the thickness of the perovskite photoactive layer used in our design is much thinner than the thickness in other works and the cathode is designed to be semitransparent to create the transmitted colors. This suggests that there is a trade-off between the power conversion efficiency and the transmission efficiency. It should also be noted that each Ag layer is preceded by a very thin organic material, PTCBI, to promote a smooth surface of an optically thin Ag film that minimizes the light scattering loss.[14,15] In addition to the smooth thin Ag film formation, the PTCBI layer, in particular interfaced with the PCBM, functions as an efficient hole blocking layer due to good energy band alignment as shown in Fig. 1 (b).

In Fig. 2 (a), the simulated (solid curves) and measured (dotted curves) spectral transmittance curves of the RGB colored perovskite PV devices at normal incidence are presented. 115, 85, and 65 nm of the WO_3 film thickness are used in order to produce RGB transmission colors, respectively, while the rest of layers' thicknesses remain the same for all colored devices as described in the caption of Fig. 1 (a). The corresponding Fabry-Perot resonances in the transmittance are 630, 540, and 450 nm, respectively. A transfer matrix method-based optical simulation was carried out based on refractive indices of all the materials measured by using a spectroscopic ellipsometer (M-2000, J. A. Woollam), which is given in the Supplementary Information. Each resonant wavelength in the measured transmittance spectra was in good agreement with that in the simulated results. On the

other hands, bandwidth and peak values of the simulated transmittances were slightly higher than those of measured ones. These discrepancies between the simulated and measured profiles get large as the wavelength increases, which is attributed to the fact that the red colored cell has the sharpest resonance among the three colored devices due to relatively small optical absorptions of the perovskite material at longer wavelengths (See the wavelength-dependent imaginary part of the refractive index of the perovskite material in the Supplementary Information). Such a sharp resonance effect (i.e., strong optical interference) can be strongly influenced by the roughness in thin films that cause the scattering and graded refractive index effect, thus rendering the resonance broad with lower efficiency. Note that our colored devices show a low transmission at around 780 nm that corresponds to the band gap of the perovskite material, which is distinctly different from what has been observed from the previously reported semitransparent perovskite solar cells.[12,27-30] Due to the low absorption coefficient of the perovkiste material at 780 nm, the transmission of the previous demonstration is always high, showing reddish transmitted colors. In our case, however, strong optical interference behaviors in the MDM multilayer structure allows incident light at off-resonance wavelengths to be destructively interfered, thus leading to strong reflections. We also note that a part of the photons in the blue spectral region of AM1.5 is transmitted, which cannot be harvested by the blue colored cell. This is responsible for the lowest short-circuit current density (J_{sc}) among the three colored devices, which will be validated by measuring a current density-voltage (J-V) characteristics later. On the other hand, the highest J_{sc} can be achieved by the red colored device since most incident solar light energy, in particular shorter wavelengths where the optical absorption of the perovskite material is fairly large, can contribute to electric power generation without much disturbance. Fig. 2 (b) exhibits optical images of the fabricated devices, showing that a background water fountain can be seen through the fabricated colored cells with distinctive RGB colors. Note that the different colors can be readily tuned by altering the thickness of the optical spacer layer (i.e., WO_3) in the MDM while keeping the other layers the same (including perovskite semiconductor), therefore the proposed approach can be easily scaled to large areas.[13]

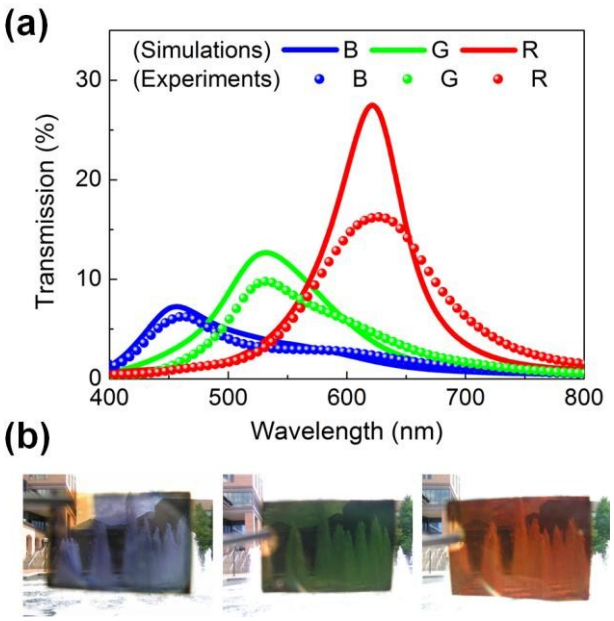

Fig. 2 (a) Simulated and measured spectral transmittance curves of the proposed colorful, see-through perovskite PV devices at normal incidence. Increasing the thickness of the WO_3 layer in the microcavity cathode allows the resonance (i.e., transmission peak) to be shifted toward the longer wavelengths. The resonances at 630 (Red), 540 (Green), and 450 nm (Blue) are attained by 115, 85, and 65 nm of the WO_3 layer thicknesses, respectively. As the wavelength increases, the difference between the simulated and measured transmission spectra becomes large. Due to the negligible absorption of the perovskite photoactive layer at longer wavelengths, the red colored PV cell has the sharpest resonance behavior that can be strongly weakened by the surface roughness. (b) Optical photographs of fabricated colored PV devices. The background image can be clearly seen through our fabricated samples with RGB colors.

Fig. 3 depicts normalized intensity distributions of the optical field of the RGB colored PV devices, each of which has different thickness of the optical spacer layer WO_3 (R: 115 nm, G: 85 nm, and B: 65 nm). In all three structures there is strong optical field intensity in the WO_3 layer inside the MDM structure, and the wavelength showing high optical field concentration in the optical spacer layer matches well with the peak position of the spectral transmittance as exhibited in Fig. 2 (a), indicating a strong Fabry-Perot resonance behavior for the three colored cells. We also note that the blue colored cell shows a lower magnitude of the optical field intensity in the MDM structure since the majority of shorter wavelengths are harvested by the perovskite photoactive layer.

The optical resonance in the MDM structure could affect the total optical interference inside the devices; hence, the light absorption at the perovskite layer is influenced as well. To elucidate how much the light absorption at the perovskite layer is changed by the optical interference effects, we focus on the absorption spectra of the photoactive layer and the corresponding photocurrent. As the photoactive layer thickness is the same and the thin Ag layer in the cathode results in a weak reflection, it is thus expected to have the similar optical absorption characteristics for the three colored devices despite the different resonance wavelength. Simulated absorption spectra in the photoactive layer of the colored solar cells are shown in Fig. 4 (a), which match well with measured external quantum efficiency (EQE) spectra depicted in Fig. 4 (b). This good agreement indicates that there is negligible charge carrier recombination, and that a conversion of the absorbed photons into photogenerated charges collected by the electrode with nearly 100% efficiency. This can be explained by the fact that a typical diffusion length of the perovskite material is much longer than the thickness of the perovskite layer used in our colored cell design.[31,32] From the measured EQE spectra, it is clear that the blue colored cell has the relatively lower EQE profiles at a blue spectral range as compared to the green and red cell devices because the resonance in the spectral transmittance at 450 nm is created for transmitting the blue color, which cannot be utilized for electric power generation, while the EQE spectrum of the red colored device is lower than that of both the blue and green colored cells at around 600 nm.

Finally we show the electrical characteristics of the microcavity-embedded perovskite PV devices. The current – voltage (J-V) measurements of the colored PV cells under simulated AM 1.5 sunlight illumination are shown in Fig. 5. The electrical performances of each colored PV cells are also summarized in the inset. As we expected, the blue colored device shows a lower J_{sc} value (6.89 mA cm^{-2}) than the green (7.08 mA cm^{-2}) and red cells (7.63 mA cm^{-2}). This is attributed to the fact that creating the transmitted resonance at the short wavelength region that corresponds to strong absorption range of the perovskite absorption causes the short wavelengths of the incident solar spectrum not to be fully harvested by the solar cell devices, thus leading to lower J_{sc} value for the blue colored device. The red colored cell shows J_{sc} of 7.63 mA cm^{-2}, an open-circuit voltage (V_{oc}) of 0.83 V and a fill factor (FF) of 61%, yielding a power conversion efficiency of 3.86%. In such a colored device configuration, J_{sc} is limited due to the requirement of transmitting a specific color. However, V_{oc} and FF could be improved by the optimization of the interface and device fabrication as for the case of conventional perovskite PV cells. We believe the design strategy described here could bring the PV cells into architectures with a wide variety of appealing design features, thus opening the potential for decorative BIPV.

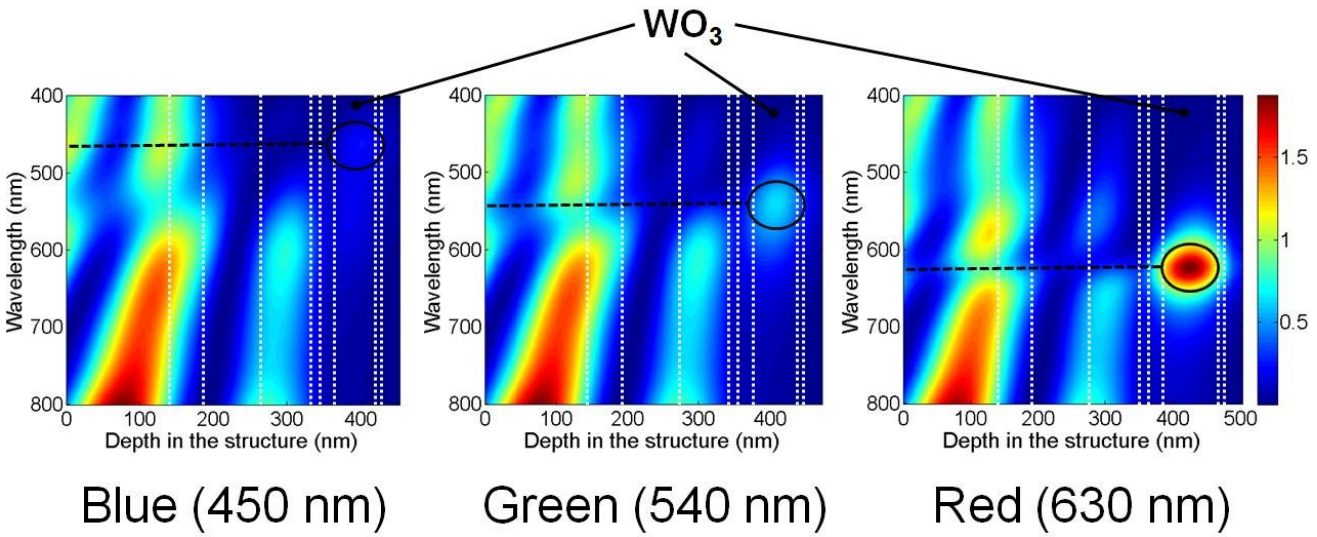

Fig. 3 Normalized optical field intensity profiles of the colored PV cells with different thickness of the WO_3 medium: 65 nm (left), 85 nm (medium), and 115 nm (right). The incident light is coming from the left-hand side and the boundary of each medium is indicated by white dotted lines. The position where the optical field is highly concentrated in the WO_3 layer corresponds to the resonance wavelength that is in good agreement with the transmission peak as shown in Fig. 2 (a).

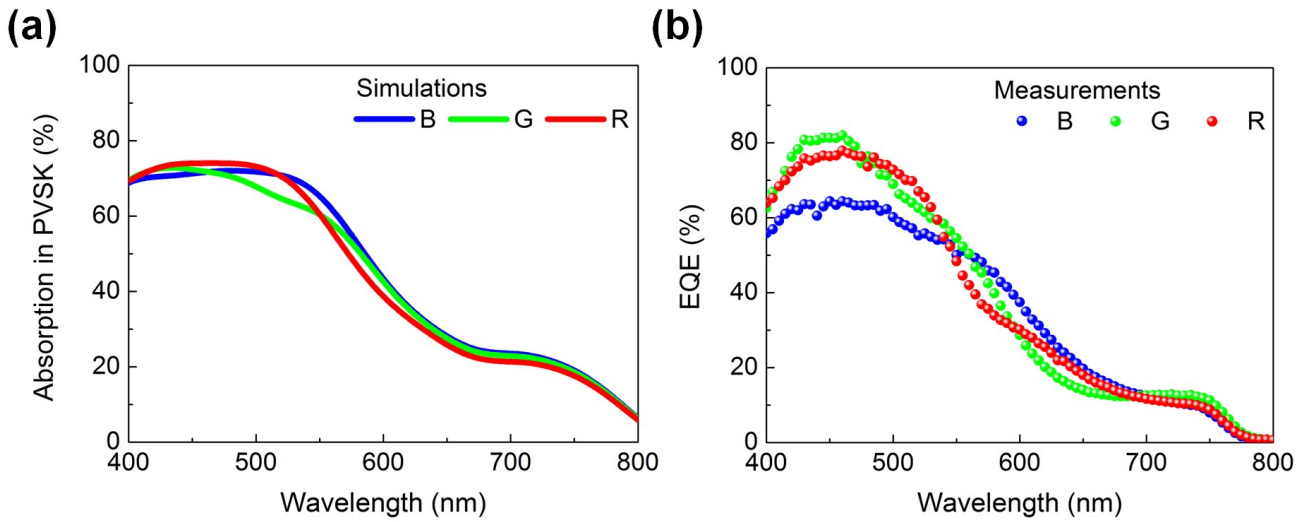

Fig. 4 (a) Simulated optical absorption spectra in the perovskite photoactive layer for three RGB individual colored PV cells. (b) The corresponding measured external quantum efficiency (EQE) profiles exhibiting relatively good agreement with the simulated results. This leads to insignificant charge carrier recombination implying that converting the absorbed photons into photogenerated charges with high efficiency is achieved.

Conclusions

In conclusion, we have demonstrated a microcavity-embedded photonic color filtering scheme integrated with perovskite PV

cells capable of transmitting distinctive colored lights. The colors can be readily tuned by varying the thickness of the optical spacer inside the composite cathode. Therefore the design principle is applicable to the entire visible wavelength range and the devices can simultaneously generate electric power with up to ~4% of power conversion efficiency. It has also been shown that greatly suppressed electron-hole recombination is enabled by the ultra-thin photoactive layer thickness as compared to the charge diffusion length of the perovskite material. This technique open the door to a number of applications, such as energy-efficient colored display systems and decorative solar panels that can be harmoniously integrated with the interior and exterior of the buildings.

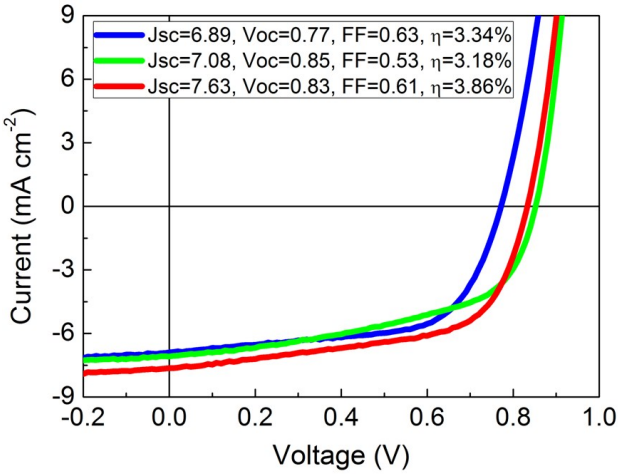

Fig. 5 Measured current density vs. voltage (J–V) characteristics of the colored semitransparent perovskite PV cell devices under a simulated AM1.5 solar spectrum illumination (100 mW cm^{-2}). The electrical performances, including J_{sc}, V_{oc}, and FF, of RGB colored PV devices are given in the inset.

Experimental section

Device fabrication and characterization

ITO coated glasses (Rs=8-12 Ω/square, Delta Technologies) were cleaned with acetone and 2-propanol for 10 minutes successively under sonication, followed by further cleaning with oxygen plasma treatment for 3 minutes. PEDOT:PSS (CLEVIOS™ AI 4083) filtered with 0.45 m NY filter were spun on ITO coated glasses at 4000 rpm for 60 seconds and annealed at 120 ℃ for 15 minutes. After the substrates were transferred to N_2 glovebox, 20wt% solution of methylammonium iodide and lead chloride (3:1 molar ratio in DMF) was spun on PEDOT:PSS at 6000 rpm for 45 seconds, followed by annealing at 80 ℃ for 3 hours. Afterward, PCBM was coated by spin coating at 800 rpm for 30 seconds. PTCBI/Ag/WO_3/PTCBI/Ag was deposited successively by a thermal evaporation with shadow masks, making the device area of 0.785 mm^2 (a circular area with the diameter of 1mm) for electrical characteristics measurement. For the optical property measurement, the samples were made without the shadow mask so that the sample size is large as shown in Fig. 2 (b). J-V measurements were performed with voltage scanning from forward bias to backward bias at 0.01 V/sec under illumination of AM 1.5 simulated sunlight.

Acknowledgement

We would like to thank NSF (ECCS 1202046) and UM-SJTU JI for the support of this work. Dr. Fukuda acknowledges the support by the Kaneka Corporation.

Notes and references

[a] *Department of Electrical Engineering and Computer Science, The University of Michigan, Ann Arbor, Michigan 48109, USA*
E-mail: guo@umich.edu

† Electronic Supplementary Information (ESI) available: [details of any supplementary information available should be included here]. See DOI: 10.1039/b000000x/

‡ These authors contributed equally to this work.

1 M. Liu, M. B. Johnston, and H. J. Snaith, *Nature*, 2013, **501**, 395-398.
2 M. A. Green, A. Ho-Baillie, and H. J. Snaith, *Nature Photon.*, 2014, **8**, 506-514.
3 J. M. Ball, M. M. Lee, A. Hey, and H. J. Snaith, *Energy Environ. Sci.*, 2013, **6**, 1739.
4 C. Wehrenfennig, M. Liu, H. J. Snaith, M. B. Johnston, and L. M. Herz, *Energy Environ. Sci.*, 2014, **7**, 2269.
5 G. E. Eperon, V. M. Burlakov, P. Docampo, A. Goriely, and H. J. Snaith, *Adv. Funct. Mater.*, 2014, **24**, 151-157.
6 B. Cai, Y. Xing, Z. Yang, W.-H. Zhang, and J. Qiu, *Energy Environ. Sci.*, 2013, **6**, 1480-1485.
7 P. Qin, S. Tanaka, S. Ito, N. Tetreault, K. Manabe, H. Nishino, M. K. Nazeeruddin, and M. Grätzel, *Nat. Commun.*, 2014, **5**, 3834.
8 H. Zhou, Q. Chen, G. Li, S. Luo, T.-b. Song, H.-S. Duan, Z. Hong, J. You, Y. Liu, and Y. Yang, *Science*, 2014, **345**, 542-546.
9 H. Yu, F. Wang, F. Xie, W. Li, J. Chen, and N. Zhao, *Adv. Funct. Mater.*, 2014, **24**, 7102-7108.
10 E. Edri, S. Kirmayer, S. Mukhopadhyay, K. Gartsman, G. Hodes, and D. Cahen, *Nat. Commun.*, 2014, **5**, 3461.
11 A. T. Barrows, A. J. Pearson, C. K. Kwak, A. D. F. Dunbar, A. R. Buckleya, and D. G. Lidzey, *Energy Environ. Sci.*, 2014, **7**, 2944-2950.
12 G. E. Eperon, V. M. Burlakov, A. Goriely, and H. J. Snaith, *ACS Nano*, 2014, **8**, 591-598.
13 H. J. Park, T. Xu, J. Y. Lee, A. Ledbetter, and L. J. Guo, *ACS Nano*, 2011, **5**, 7055-7060.
14 K.-T. Lee, J. Y. Lee, S. Seo, and L. J. Guo, *Light: Sci. & Appl.*, 2014, **3**, e215; DOI:10.1038/lsa.2014.96.
15 J. Y. Lee, K.-T. Lee, S. Seo, and L. J. Guo, *Sci. Rep.*, 2014, **4**, 4192; DOI:10.1038/srep04192.
16 M. Fukuda, K.-T. Lee, J. Y. Lee, and L. J. Guo, *IEEE J. Photovolt.*, 2014, **4**, 1337-1342.
17 M. A. Kats, R. Blanchard, P. Genevet, and F. Capasso, *Nature Mater.*, 2013, **12**, 20–24.
18 K.-T. Lee, S. Seo, J. Y. Lee, and L. J. Guo, *Adv. Mater.*, 2014, **26**, 6324-6328.
19 M. A. Kats, D. Sharma, J. Lin, P. Genevet, R. Blanchard, Z. Yang, M. M. Qazilbash, D. N. Basov, S. Ramanathan, and F. Capasso, *Appl. Phys. Lett.*, 2012, **101**, 221101.
20 K.-T. Lee, S. Seo, J. Y. Lee, and L. J. Guo, *Appl. Phys. Lett.*, 2014, **104**, 231112.
21 M.-G. Kang, H. J. Park, S.-H. Ahn and L. J. Guo, *Sol. Energ. Mat. Sol. C.*, 2010, **94**, 1179-1184.
22 M. G. Kang, T. Xu, H. J. Park, X. G. Luo, and L. J. Guo, *Adv. Mater.*, 2010, **22**, 4378-4383.
23 C. Zhang, D. Zhao, D. Gu, H. Kim, T. Ling, Y.-K. R Wu, and L. J. Guo, *Adv. Mater.*, 2014, **26**, 5696-5701.
24 S. Schubert, J. Meiss, L. Müller-Meskamp, and K. Leo, *Adv. Energy Mater.*, 2013, **3**, 438-443.
25 C.-C. Chueh, S.-C. Chien, H.-L. Yip, J. F. Salinas, C.-Z. Li, K.-S. Chen, F.-C. Chen, W.-C. Chen and A. K.-Y. Jen, *Adv. Energy Mater.*, 2013, **3**, 417–423.

26 K. Hong, K. Kim, S. Kim, I. Lee, H. Cho, S. Yoo, H. W. Choi, N.-Y. Lee, Y.-H. Tak, and J.-L. Lee, *J. Phys. Chem. C*, 2011, **115**, 3453–3459.
27 C. Roldan-Carmona, O. Malinkiewicz, R. Betancur, G. Longo, C. Momblona, F. Jaramillo, L. Camachob, and H. J. Bolink, *Energy Environ. Sci.*, 2014, **7**, 2968-2973.
28 L. K. Ono, S. Wang, Y. Kato, S. R. Raga, and Y. Qi, *Energy Environ. Sci.*, 2014, **7**, 3989-3993.
29 G. E. Eperon, D. Bryant, J. Troughton, S. D. Stranks, M. B. Johnston, T. Watson, D. A. Worsley, and H. J. Snaith, *J. Phys. Chem. Lett.*, 2015, **6**, 129–138.
30 F. Guo, H. Azimi, Y. Hou, T. Przybilla, M. Hu, C. Bronnbauer, S. Langner, E. Spiecker, K. Forberich, and C. J. Brabec, *Nanoscale*, 2015, **7**, 1642-1649.
31 S. D. Stranks, G. E. Eperon, G. Grancini, C. Menelaou, M. J. P. Alcocer, T. Leijtens, L. M. Herz, A. Petrozza, and H. J. Snaith, *Science*, 2013, **342**, 341-344.
32 G. Xing, N. Mathews, S. Sun, S. S. Lim, Y. M. Lam, M. Grätzel, S. Mhaisalkar, and T. C. Sum, *Science*, 2013, **342**, 344-347.

Table of Contents

Optical cavity-integrated perovskite solar cells capable of creating distinctive semitransparent colors with high efficiencies are demonstrated.